

Author Manuscript

This is the author manuscript accepted for publication and has undergone full peer review but has not been through the copyediting, typesetting, pagination and proofreading process, which may lead to differences between this version and the [Version of Record](#). Please cite this article as [doi: 10.1111/mec.15357](https://doi.org/10.1111/mec.15357)

This article is protected by copyright. All rights reserved

1
2 DR. ANDRÉA T. THOMAZ (Orcid ID : 0000-0002-9755-2674)

3
4
5 Article type : Original Article

6
7
8 **Original article**

9
10 **Title:** Common barriers, but temporal dissonance: genomic tests suggest ecological and paleo-
11 landscape sieves structure a coastal riverine fish community

12
13 **Running title:** Ecological and paleo-landscape sieves in fish

14
15 **Authors:** Andréa T. Thomaz^{1,2}, L. Lacey Knowles¹

16 ¹ Department of Ecology and Evolutionary Biology, University of Michigan, Ann Arbor MI, USA
17 48109.

18 ² Biodiversity Research Centre and Department of Zoology, University of British Columbia,
19 Vancouver, BC, Canada, V6T 1Z4

20
21 Corresponding author:

22 Andréa T. Thomaz, thomaz@biodiversity.ubc.ca, +1(778)316-9657

23 Biodiversity Research Centre and Department of Zoology

24 University of British Columbia

25 2212 Main Mall

26 Vancouver, BC – Canada V6T 1Z4

27

28 Word count: 6,737

Author Manuscript

29 **Abstract**

30 Assessments of spatial and temporal congruency across taxa from genetic data provide
31 insights into the extent to which similar processes structure communities. However, for coastal
32 regions that are affected continuously by cyclical sea-level changes over the Pleistocene,
33 congruent interspecific response will not only depend upon co-distributions, but also on similar
34 dispersal histories among taxa. Here, we use SNPs to test for concordant genetic structure among
35 four co-distributed taxa of freshwater fishes (Teleostei: Characidae) along the Brazilian Atlantic
36 coastal drainages. Based on population relationships and hierarchical genetic structure analyses,
37 we identify all taxa share the same geographic structure suggesting the fish utilized common
38 passages in the past to move between river basins. In contrast to this strong spatial concordance,
39 model-based estimates of divergence times indicate that despite common routes for dispersal,
40 these passages were traversed by each of the taxa at different times resulting in varying degrees
41 of genetic differentiation across barriers with most divergences dating to the Upper Pleistocene,
42 even when accounting for divergence with gene flow. Interestingly, when this temporal
43 dissonance is viewed through the lens of the species-specific ecologies, it suggests that an
44 ecological sieve influenced whether species dispersed readily, with an ecological generalist
45 showing the highest propensity for historical dispersal among the isolated rivers of the Brazilian
46 coast (i.e., the most recent divergence times and frequent gene flow estimated for barriers). We
47 discuss how our findings, and in particular what the temporal dissonance, despite common
48 geographic passages, suggest about past dispersal structuring coastal communities as a function
49 of ecological and paleo-landscape sieves.

50

51 **Keywords:** Atlantic Rainforest, coastal drainages, freshwater fishes, Pleistocene, population

52 turnover, sea-level fluctuations

Author Manuscript

53 **Introduction**

54 Spatial congruence in the distribution of species or in their genetic structure has long been
55 recognized as a signal of shared evolutionary history (Bermingham & Avise, 1986; Donoghue &
56 Moore, 2003; Edwards & Beerli, 2000). Such congruence has helped to identify geographical
57 features structuring communities, especially in cases where a physical barrier is not readily
58 evident, such as ephemeral, climatic and ecological barriers (Avise, 1992; Carnaval, Hickerson,
59 Haddad, Rodriguez, & Moritz, 2009; Edwards, Keogh, & Knowles, 2012), or when genetic
60 discontinuities are a function of dispersal and demographic traits (Irwin, 2002).

61 Although concordant genetic structure is strong evidence of a shared evolutionary history
62 among co-occurring taxa, the lack of concordance has different possible explanations that can
63 limit the insights genetic tests alone can provide (Papadopoulou & Knowles, 2016). For example,
64 at regional scales, geological constraints tend to prevail over possible species-specific responses
65 (Albert & Carvalho, 2011; Bermingham & Avise, 1986; BurrIDGE, Craw, & Waters, 2006;
66 Chakona, Swartz, & Gouws, 2013). However, for dynamic histories, such as those subject to
67 cyclical climatic changes, complex colonization and extinction dynamics, and hence,
68 incongruence among community members (e.g., Burbrink et al., 2016) pose specific challenges
69 for understanding the processes underlying genetic structuring. This lack of similarity has left
70 researchers with unanswered questions about how different species respond to potential routes of
71 dispersal among currently isolated populations (Massatti & Knowles, 2016).

72 In our study, we focus on a coastal riverine fish community of the Brazilian Atlantic
73 Rainforest and take advantage of the dispersal constraints imposed upon riverine fishes to test the
74 community response to historical connections among isolated basins that affect species
75 distributions and dispersal in coastal environments (Dias et al., 2014). That is, unlike terrestrial

76 systems in which genetic structure reflects the effects of habitat suitability in the past or present
77 landscape on movement patterns (see He, Edwards, & Knowles, 2013; López-Urbe, Jha, & Soro,
78 2019), for riverine species, dispersal is restricted to physical connections across riverine basins
79 (Albert, Petry, & Reis, 2011). As such, the degree of genetic structure across isolated basins
80 reflects the extent to which dispersal has been historically limited. Likewise, similarity in the
81 spatial genetic structure across multiple species identifies routes of connectivity that were
82 accessible to multiple members of aquatic communities, although they may, or may not, have
83 been traversed at similar times (i.e., the divergence times associated with similar spatial structure
84 may differ across taxa).

85 By coupling spatial and temporal tests of congruent genetic structure with consideration
86 of the ecological differences among four focal taxa distributed along the coastal Atlantic
87 Rainforest, we consider how both the paleo-landscape (e.g., past riverine connectivity) and the
88 ecology of the taxa themselves might act as sieves – that is, determine when and which taxa
89 moved between current isolated river basins. As a consequence of repeated population cycles of
90 isolation and reconnection during the Pleistocene (Papadopoulou & Knowles, 2016; Thomaz &
91 Knowles, 2018), coastal areas may be subject to high spatial and/or temporal lineage turnover
92 (e.g., extirpation-isolation-recolonization; Dolby, Ellingson, Findley, & Jacobs, 2018). Such
93 turnover may contribute to the lack of congruent genetic structure. Moreover, even with
94 congruent spatial genetic structure, there might not be temporal congruence because connections
95 among isolated regions were forged repeatedly, and at different times, during periods of low sea
96 level. Specifically, temporary passages (e.g., river captures and/or riverine connections when sea-
97 level retreat; Lima et al., 2017; Thomaz, Malabarba, & Knowles, 2017; Weitzman, Menezes, &

98 Weitzman, 1988) may not be effectively utilized by all species because species-specific
99 ecological differences might make some routes more or less accessible to some taxa.

100 To address these questions, we studied four co-distributed characid taxa (Ostariophysi:
101 Characiformes), commonly known as tetras, distributed along the Brazilian coast that differ
102 ecologically (Figure 1). Specifically, the focal taxa span a spectrum of ecological specialization
103 and differ in their distance from the current coastline (i.e., areas of proposed connections among
104 currently isolated basins; Conti & Furtado, 2009; Thomaz & Knowles, 2018). They include the
105 more generalized taxon *Mimagoniates microlepis* that inhabits lowland and highland rivers, and
106 *Hyphessobrycon boulengeri*, which is restricted to lowland rivers, as well as *Hollandichthys*,
107 which is restricted to rivers surrounded by a dense forest canopy, and the coastal *Bryconamericus*
108 species group (and hereafter referred as *Bryconamericus*) that inhabits the fast-moving waters of
109 rivers on steep slopes (Figure 1; see Supplement Text S1 for taxonomic details). By testing for
110 spatial congruence and assessing the relative timing of divergence in a comparative framework,
111 our study provides insights about the ecological and paleo-landscape sieves that structure this
112 coastal fish community. We also discuss the implications of our results for more general patterns
113 of species distributions and population connections in coastal communities, including a
114 comparison with terrestrial counterparts in the Brazilian Atlantic rainforest.

115

116 **Material and Methods**

117 Sampling and genomic data

118 Specimens for each of the four species were collected across their entire distributions;
119 collecting expeditions were conducted during different seasons, with collections of the four taxa
120 concentrated during the 2008-2009, and 2013-2015 field seasons. A total of 47 drainages

121 (populations) were sampled across the four taxa, with an average of 23 drainages sampled per
122 species (Table S1). Vouchers and tissues for this study were catalogued in the ichthyology
123 collection at the Universidade Federal do Rio Grande do Sul (UFRGS), Brazil. Detailed
124 information about fieldwork and vouchers specimens can be obtained from each catalog number
125 using <http://sblink.cria.org.br/>. Collection permits were obtained with the Brazilian government
126 through the Instituto Chico Mendes de Conservação da Biodiversidade (ICMBio), under the
127 license #12038 for Dr. Luiz R. Malabarba at Universidade Federal do Rio Grande do Sul - Brazil.
128 Additional tissues (approximately 10% of the samples) were obtained from the Museu the
129 Ciências e Tecnologia, Pontifícia Universidade Católica do Rio Grande do Sul (MCP) and Museu
130 the História Natural Capão da Imbuia (MHNCI) (see complete list in Table S2). All specimens
131 and tissues used in this study are in accordance with the Brazilian genetic patrimony rules and
132 indexed in the SISGEN database under the number RF0AF3D.

133 Six double digest Restriction-site Associated DNA (ddRAD) libraries were constructed:
134 three libraries contained 118 individuals of *Mimagoniates microlepis* for this study (the other 132
135 individuals sequenced across these libraries were for an unrelated study that is currently
136 unpublished), two libraries containing 136 individuals of *Hyphessobrycon boulengeri*, and one
137 library with 87 individuals of *Bryconamericus*. In addition, two libraries with 182 individuals of
138 *Hollandichthys* were re-analyzed for this study (Thomaz et al., 2017). For some of these nominal
139 taxa, our sampling encompasses more than a single species given taxonomic treatments (see
140 Supplement Text S1 for details). Here we opt to refer to each taxon by the designations identified
141 above because we note that our results are robust given that the proposed taxonomic revisions all
142 pertain to allopatric lineages, and therefore do not confound our analysis of spatial or temporal
143 congruence/discord (see discussion section for additional detail).

144 For all the libraries prepared specifically for this study, we followed the protocol of
145 Peterson, Weber, Kay, Fisher, & Hoekstra (2012); the two previously sequenced libraries of
146 *Hollandichthys* followed the Parchman et al. (2012) protocol (see Thomaz et al., 2017 for
147 preparation details), but with the main features are in common with the other protocol (e.g., the
148 enzymes used and size selection). Briefly, genomic DNA was extracted using Qiagen DNeasy
149 kits from tissue samples taken from alcohol preserved body muscle. Between 300 and 400ng of
150 each DNA sample was double digested with two restriction enzymes (EcoRI and MseI), followed
151 by a ligation step to add unique barcodes. Samples for each library were pooled and fragments
152 between 350-450bp were selected using a PippinPrep. A PCR with 10 cycles was used to add
153 Illumina flowcell adapters. All steps described above were followed by a clean-up step using
154 AMPure beads (1.6x ratio; except after Pippin Prep) to remove small DNA fragments such as
155 primers, and by a high sensitivity Qubit quantification assay. Libraries were sequenced on an
156 Illumina HiSeq2500 to generate single-end 150bp reads (100bp for *Hollandichthys*) at The Centre
157 for Applied Genomics, Toronto, Canada.

158 Genomic data were demultiplexed and processed separately for each taxon with the
159 STACKS version 1.41 pipeline (Catchen, Hohenlohe, Bassham, Amores, & Cresko, 2013). For
160 quality filtering, reads with more than one mismatch in the adapter sequence or a barcode
161 distance greater than two (as specified in process radtags) were removed, and individuals with
162 less than 300K reads were excluded. To create stacks within each sample, USTACKS was run
163 with a minimum depth of coverage of five and an error bound of $\epsilon = 0.1$, followed by CSTACKS
164 with a maximum of two mismatches between sequences within a given stack in order to build a
165 catalog of all loci. The stacks of individual samples were matched against the catalog using
166 SSTACKS with default options. To obtain a vcf output file containing all variable sites from

167 STACKS, we ran the POPULATIONS module with “loose” parameters (i.e., -r 0 -p 2 -m 5 --
168 min_maf 0 --max_obs_het 0.5). We processed this output file in R version 3.3.1 (R Core Team,
169 2018) to create a whitelist that excluded highly variable positions at the 3’ end of all locus and
170 loci with θ -values above the 95th percentile of this distribution, to avoid errors associated with
171 sequencing and assembly (see Figures S1 and S2). Using this whitelist, we re-ran the
172 POPULATIONS module. All bioinformatics processing with STACKS was performed in the
173 Advanced Research Computing Technology Services at the University of Michigan. We obtained
174 a total of 165 million to 325 million reads per species.

175 Because of the various requirements of different analyses used to characterize the
176 geographic structuring of genomic variation, such as sensitivity to missing data (Huang &
177 Knowles, 2016a) and for computational feasibility, three datasets were generated varying the
178 amount of missing data and the numbers of individuals. One dataset was comprised by one
179 random single SNP per locus with maximum of 50% missing data, and hereafter referred to as the
180 SNP dataset (see Table S3 for details), which was used for estimates of population trees; a
181 population refers to all the samples from the same river basin/drainage (or island - see Table S2).
182 The other dataset included loci with maximum 25% missing data after filtering and hereafter
183 referred to simply as the genomic dataset. Note that for *M. microlepis* we allowed 35% missing
184 data because of the higher levels of missing data that resulted from the addition of individuals in
185 the preparation of the library (specifically, samples from a southern population unrelated to this
186 project were included). The genomic dataset was used in most of the analyses including the
187 calculation of summary statistics in the POPULATIONS module of STACKS, whereas a random
188 single SNP per locus were used in the STRUCTURE analysis. Separate datasets, hereafter
189 referred as the reduced datasets, were used in FASTSIMCOAL2 analyses and were generated,

190 when possible, from 20 individuals with the smallest amount of missing data from all the
191 populations separated by each geographic barrier for each taxon (40 individuals in total; see
192 Table S1 for number of individuals used per population), and a single variable SNP per RADtag
193 with less than 10% missing data (see details below). For all these datasets, individuals with
194 considerably fewer SNPs in comparison to other individuals of the same population were
195 excluded. All filtering steps were performed using the toolset PLINK v.1.90 (Purcell et al., 2007;
196 no filter to screen potentially selected loci was applied given the difficulties of inferring selection
197 under the structured populations). [Genomic data are archived on SRA \(BioProjectID: PRJNA](#)
198 [598706\)](#) and all scripts and setting files for programs are available on Dryad under doi:
199 [10.5061/dryad.zkh18936g](#) and on GitHub:
200 https://github.com/ichthya/ThomazKnowles2020_scripts. After applying filters for missing data,
201 genotyping rates ranged from 0.67 to 0.72 for the SNP dataset and from 0.85 to 0.92 for the
202 genomic dataset across species (see Table S2 and S3 for information per individuals and per
203 species, respectively).

204

205 Characterizations of population structure

206 To examine evolutionary relationships among populations from the drainages along the
207 Brazilian coast, we estimated a population tree (Knowles & Cartens, 2007), accounting for the
208 coalescent variation associated with random sorting of gene lineages among loci, and incomplete
209 lineage sorting for any given locus, using the program SVDquartets (Chifman & Kubatko, 2014)
210 and as implemented in PAUP* 4.0 (Swofford, 2003) under the multispecies coalescent model
211 with all possible quartets evaluated. Branch support was assessed with 1,000 bootstrap replicates
212 and midpoint rooting was used given the absence of outgroups in our datasets.

213 Hierarchical STRUCTURE analyses (Pritchard, Stephens, & Donnelly, 2000) were used to
214 evaluate if the probabilistic assignment of individuals in each taxon to genetic clusters showed a
215 species-specific geographic configuration or if there is a general pattern shared among taxa along
216 the Brazilian coast. Specifically, to assess substructure, we performed analyses with the full
217 distribution of a taxon followed by sequential analyses for each of the subsets identified as
218 distinct genetic clusters (see Massatti & Knowles, 2014). The genomic datasets with a single SNP
219 per locus were used, and individuals were not conditioned on any population membership (i.e.,
220 population membership was not used as priors). Each dataset was analyzed with K-values ranging
221 from 1 to 5 or 10 (see Table 1 for specific information for each species). We performed ten
222 independent runs under the “Admixture” and “Allele Frequencies Correlated” models for 500,000
223 MCMC iterations following a burn-in period of 200,000 iterations for each analysis. The ΔK of
224 Evanno, Regnaut, & Goudet (2005) implemented in STRUCTURE HARVESTER (Earl &
225 vonHoldt, 2012) was used to identify for each taxon the most likely number of genetic clusters.
226 We also considered the likelihood-values for $K = 1$ and 2 to evaluate the lack of geographic
227 structure. The graphical probabilistic assignment of individuals to clusters performed using the
228 CLUMPAK pipeline (Kopelman, Mayzel, Jakobsson, Rosenberg, & Mayrose, 2015).

229
230 Tests of divergence models

231 Focusing on the genetic clusters identified among the different taxa based on the
232 phylogenetic tree and STRUCTURE analyses, we performed model comparisons to estimate
233 divergence times and the frequency and strength of connectivity among each geographic barrier
234 for each taxon separately using the composite-likelihood method FASTSIMCOAL2 (Excoffier &
235 Foll, 2011; Excoffier, Dupanloup, Huerta-Sánchez, Sousa, & Foll, 2013) based on the folded

236 joint Site Frequency Spectrum (SFS; i.e., for the minor allele since we do not have information
237 from outgroups to obtain the derived state; Figure S3). With the objective to maximize the
238 number of loci with no missing data and obtain an accurate estimation of allelic frequencies for
239 calculating the SFSs, each SFS was built by subsampling 15 individuals per locus (out of 20
240 individuals from the reduced datasets; see Table S5 for exceptions) from either side of each
241 geographic barrier using a custom script; the script is available on GitHub:
242 <https://github.com/ichthya> and is modified from He & Knowles (2016).

243 Based on each SFS, we estimated parameters under three classes of divergence models:
244 (1) divergence without gene flow (herein called “strict divergence”), and two models of
245 divergence with gene flow, namely (2) divergence with unconstrained gene flow (i.e., gene flow
246 could occur throughout the divergence history, and herein is called “*divergence with gene flow*”),
247 and (3) divergence with gene flow as a single pulse (herein called “*divergence with a pulse of*
248 *gene flow*”). For each of the divergence with gene flow models, symmetrical versus asymmetrical
249 gene flow was modeled (i.e., models with one versus two migration parameters). The variety of
250 models of gene flow were chosen to accommodate differences in how frequently connections
251 might have been forged between the current isolated river basins, and hence potential differences
252 in how gene flow among populations might have occurred, which is central to testing the
253 hypothesis that species-specific traits might affect how effective a barrier might be (i.e., whether
254 species were more or less likely to remain isolated for extended periods of time despite repeated
255 opportunities for gene flow via historical connections among the current isolated basins). To
256 improve the performance of parameter estimates from the SFS (following recommendations of
257 the program; see Excoffier & Foll, 2011), we calculated an effective population size of one of the
258 two populations (specifically, N_1) directly from empirical data from the nucleotide diversity (π) of

259 fixed and variable sites. The remaining parameters (i.e., N_2 , ancestral population size N_{ANC} and
260 divergence time T_{DIV} for all models, gene flow estimates, MIG as single parameter or two
261 parameters, as well as the time of gene flow, T_{GF} , in the case of the model with pulsed gene flow)
262 were estimated based on the SFS, with a mutation rate, μ , estimated from the size of a genome
263 (see formula in Lynch, 2010) based on a close relative for each species (see Table 2 and S5 for
264 details). To control for the sensitivity of our estimated divergence times to different settings of μ ,
265 we also repeated the analyses using the same mutation rate across the species; specifically, we
266 used the mean μ among all four species ($2.19E-8$). A generation time of one year was used for all
267 species, which is the common generation time in characids (Azevedo, 2010). FASTSIMCOAL2
268 runs were performed with 40 replicates for each group pair with 100,000 to 250,000 simulations
269 per likelihood estimation based upon a stopping criterion of 0.001, and 10 to 40 expectation-
270 conditional cycles (ECM). Model comparisons were performed on the basis of their likelihoods
271 using the Akaike Information Criteria (AIC; Akaike, 1974). The power to estimate the parameters
272 was assessed for the most probable model inferred for each geographic barrier and taxon by
273 performing 100 parametric bootstraps of simulated SFS; specifically, data were simulated under
274 the parameters with the highest maximum likelihood and the simulated data sets were analyzed;
275 parameters were estimated from the simulated datasets from 40 runs of each of the 100 simulated
276 SFS, and reported here as the 95% confidence interval.

277

278 **Results**

279 Population genetic structure

280 Genetic diversity estimates were generally similar across species (see Table S3), ranging
281 from *Bryconamericus*, which showed the highest genetic diversities, to *M. microlepis* and *H.*

282 *boulengeri* with lower diversities. There is also a strong correspondence between geography and
283 genetic differentiation in all four taxa. Specifically, a latitudinal pattern of relatedness is evident
284 from the phylogenetic analyses (Figures 2 and S5), except for a couple of populations of
285 *Bryconamericus* where geographically distant populations were closely related.

286 Analyses of the full dataset in STRUCTURE identified $K = 2$ as the most probable value
287 of K based on ΔK (Evanno et al., 2005) in three taxa (*M. microlepis*, *Hollandichthys*, and
288 *Bryconamericus*), and a $K = 4$ for *H. boulengeri* (Table 1). These results, as with estimated
289 phylogenetic trees, identified a geographic division in the center of the species distributions at the
290 Paranaguá estuary (hereafter referred to as the central division). This central division is apparent
291 in all four taxa, separating a northern and southern region, but in *Bryconamericus* it appears some
292 gene flow has occurred between geographically distant populations (Figure 2D).

293 Subsequent STRUCTURE analyses performed in the northern and southern regional
294 groups to account for the hierarchical structure identified $K=2$ as the most probable value in each
295 taxon (no hierarchical analysis was performed for *H. boulengeri*, given $K = 4$); note that the
296 likelihoods for $K=1$ were substantially smaller than $K=2$ in all cases (outputs available on Dryad).
297 In the northern region, the two broadly distributed taxa, *M. microlepis* and *H. boulengeri*, share a
298 geographic division above the mouth of the Paraíba do Sul River (hereafter referred to as the
299 northern division). This division is generally coincident with the northern extent of the
300 distribution of *Hollandichthys* and *Bryconamericus*, which have smaller distributional ranges.
301 These two taxa also exhibit substructure within the northern extent of their geographic range
302 (Figure 2C-D), but their limited distributions means that congruence of the northern division can
303 only be evaluated in *M. microlepis* and *H. boulengeri*. Analysis of the region south of the central
304 division identified additional congruent substructure across all four taxa (hereafter referred to as

305 the southern division), but with some spatial uncertainty. Specifically, for *M. microlepis* and
306 *Hollandichthys* the southern division occurs between Araranguá (population 6) and D'Una
307 (population 7) river basins, whereas in *Bryconamericus* the precise position cannot be assigned
308 due to a sampling gap, and in *H. boulengeri* the southern division occurs slightly to the north
309 between the island population of Florianópolis (population 9) and the inland Itajaí river basin
310 (population 12; Figure 1). All the inferred genetic clusters show a correspondence with the clades
311 in the estimated phylogenetic trees (Figure 2).

312

313 Comparisons of divergence models

314 For all the taxa and for each geographic barrier, divergence with gene flow (Table 2)
315 provided a better fit than divergence in isolation (Table S4). Whether a model with, or without,
316 pulsed gene flow was inferred as the best fit varied by taxa (Table 2). Specifically, the fit of the
317 divergence with gene flow (rather than pulsed gene flow) model was consistently estimated to be
318 a better fit in *M. microlepis* and in one case for *H. boulengeri*; however in one case – the North
319 geographic barrier in *M. microlepis* - the fit of the data did not differ substantially between the
320 two different models of gene flow (Table S4).

321 Estimates of the divergence times for each of the three inferred geographic divisions date
322 to the Upper Pleistocene (<126 kya; Figure 3) in all species, except for the Central and North
323 divisions in *H. boulengeri* (~234 and 143 kya, respectively). However, the timing of divergence
324 differs across taxa, despite spatial congruence of the geographic divisions (Figure 3 and Table 2).
325 Geographic isolation appears to correspond to at least two temporal events for each of the
326 regional divisions when we consider both the point estimates and the confidence intervals for the
327 divergence time estimates (Figure 3), irrespectively of whether genetic divergence occurred with

328 or without gene flow (Table 2 and Table S5). For example, in the northern division, the
329 divergence time in *H. Boulengeri* (~143 kya) contrasts with *M. microlepis* (divergence of ~28
330 kya; Figure 3). Likewise, the most recent estimated divergence times across taxa were ~8 and 14
331 kya for *M. microlepis* and *Hollandichthys*, suggesting observed genetic differences accumulated
332 very recently across the shared southern division, which contrast with *Bryconamericus* (~89 kya;
333 Figure 3) for this same area. Although the timing of divergence reflects when the species became
334 more or less isolated, evaluation of the best fit divergence model indicates the observed genetic
335 differentiation has accumulated with limited gene flow (i.e., divergence models with some gene
336 flow fit the data better; Table 2 and S5). When the best model was one in which gene flow
337 occurred as a single pulse, the timing of gene flow is estimated to have occurred sometime close
338 to the Last Glacial Maxima (i.e., always less than 30 kya; Table 2). Note that even though
339 divergence with gene flow provided the best fit, gene flow was insufficient to overcome the
340 genetic structure associated with the barriers in all cases.

341 Although the absolute value of the estimated divergences times and times of gene flow
342 pulses presented here might be subject to errors associated with species-specific differences of μ
343 used in the calculations, repeating the analyses using the same mutation rate across taxa
344 demonstrates our results are robust (Table 2). That is, the timing of divergence associated with
345 the barriers differed across taxa (Figure 3), despite spatial congruence in the patterns of
346 geographic isolation among the taxa (Figure 2).

347

348 **Discussion**

349 Despite shared regional genetic structure across species (Figure 2), differences in the
350 timing of divergences (Figure 3), as well as specifics regarding the limited gene flow that

351 accompanied divergence (Table 2), highlight species-specific dispersal histories. Together the
352 spatial congruence and temporal dissonance reveals the varying degrees of the ephemerality of
353 barriers across landscapes (in this case, isolated coastal riverine basins). Such regional differences
354 in connectivity across paleo-landscapes and among taxa highlight the need for a more nuanced
355 approach for understanding the processes structuring divergence in riverine communities,
356 especially for those characterized by repeated and frequent connections forged by sea-level shifts
357 associated with climatic change. In addition, our work paints a different picture than is frequently
358 envisioned about the effects of climate-induced distributional shifts in the Atlantic Forest (at least
359 for the terrestrial counterparts of the ichthyofauna) where the idea of congruent community
360 response has been popularized. Below we discuss what our findings imply about divergence
361 histories of dynamic landscapes with strict constraints on the geography of dispersal with regards
362 to both (i) the ephemerality of isolation in shaping communities during periods of dramatic
363 climate change, and (ii) expectations for similarity across taxa because of an emphasis on isolated
364 areas, as opposed to dispersal via temporary connections that may be mediated by species-
365 specific ecologies.

366
367 Ephemeral isolation driven by episodic dispersal
368 Shared haplotypes and patterns of relatedness between neighboring river basins has classically
369 been used to infer biogeographic histories shaped by past connectivity (e.g., river capture; Swartz,
370 Chakona, Skelton, & Bloomer, 2014; Lima et al., 2017), and has been extended to expectations of
371 congruence among community members (Albert et al., 2011). However, our data shows that a
372 community history shaped by a singular historical event is an oversimplification. In fact, despite

373 the obvious constraints on aquatic dispersal to water, the dispersal and the histories of community
374 members shaped by past connectivity are anything but simple (Figure 3; Table 2).

375 When we consider shared geographic divisions among taxa, the question becomes what
376 makes these regions stand out in terms of their effectiveness as barriers? Two of the three
377 geographic divisions are associated with areas of prominent mountainous relief of granite-gneiss
378 crystalline basement, which agrees with areas associated with paleodrainages boundaries (i.e., the
379 elevated boundary between two areas that drain to different river systems; Thomaz & Knowles,
380 2018; Weitzman et al., 1988). Specifically, the northern division corresponds with the Cabo Frio
381 Magmatic Lineament, and the southern division with the Serra do Tabuleiro (Villwock, Lessa,
382 Suguiu, Angulo, & Dillenburg, 2005; Zalán & Oliveira, 2005). These geologic features and
383 paleodrainages have notably been invoked as barriers contributing to both speciation and faunal
384 turnover in distributional patterns (Abell et al., 2008; Bizerril, 1994; Pereira et al., 2013; Dias et
385 al., 2014). We note that other paleodrainages have been inferred along the Brazilian coast
386 (Thomaz & Knowles, 2018), but they do not appear to be contributing equally to the regional
387 genetic differentiation across the studied taxa. Additional geological evidence could help explain
388 the why some, but not all, paleodrainages are associated with gene divergence. However, one
389 possible explanation may be that the genetic divergence associated with the two specific
390 paleodrainage boundaries detected across the four taxa studied here reflect their stability,
391 especially given that they are associated with prominent geological features that might make them
392 more likely to withstand strong erosion caused by periods of sea level change. On the other hand,
393 the lack of evidence for a role of geologic uplift associated with the central division (Figure 2) is
394 puzzling, but we note that it is positioned in an active tectonic area (i.e., Ponta Grossa Arch;
395 Ribeiro, 2006) with rivers draining to a common outlet based on paleodrainages reconstructions

396 for the LGM (Thomaz & Knowles, 2018). Although this central division has not been identified
397 for structuring communities, high genetic differentiation has been inferred in analyses of
398 population variation in other studies (Thomaz, Malabarba, Bonatto, & Knowles, 2015; Tschá et
399 al., 2017).

400 Instead of seeking spatial characteristics intrinsic to the shared regional divisions to
401 understand the distribution of genetic divergence, we might also approach the question by asking
402 why the connections forged among some, but not all, contemporary isolated basins have been
403 traversed even more recently than the three divisions identified here. Note that any isolation
404 associated among the basins contained within the inferred regional genetic groups (see Figures 2
405 and S4) is necessarily more ephemeral (i.e., it is not as old) as the shared regional geographic
406 divisions (Figure 3). It is possible that different degrees of connectivity, or conversely isolation,
407 might relate to bathymetric differences (e.g., continental shelf width and its slope) and/or
408 differences in habitat suitability (distribution of habitat over time), as is often invoked when
409 studying connectivity in terrestrial communities on islands (Ali & Aitchison, 2014; Papadopoulou
410 & Knowles, 2015, 2016; Shaw & Gillespie 2016), estuarine fishes (Dolby et al., 2018), and the
411 geographic ranges of freshwater fishes (Carvajal-Quintero et al., 2019). Given the regional
412 structure (Figure 2), we can rule out the possibility that the fish did not have sufficient time to
413 colonize these basins (i.e., each of the species at some point would have been distributed within
414 these regions). This suggests that differences in population persistence, especially given observed
415 distributional gaps within the range of some taxa (Figure 1), might contribute to local, but
416 ephemeral genetic structure. This high turnover is also supported by many freshwater fish species
417 diversity patterns in the area, which is characterized by high levels of endemism (ranging from

418 67- 95%; Bizerril, 1994; Reis et al., 2016), with small, disjunct distributions among related taxa
419 separated by some relatively depauperate areas (Ribeiro, Lima, Riccomini, & Menezes, 2006).

420 In addition to a focus on explaining where geographic barriers might arise, another and
421 relatively understudied question is whether spatial congruence of genetic divergence reflects a
422 single response by the community. To address this question, we can turn to the timing of
423 divergence across species. Overall, the genetic signal recovered here indicates that older events
424 would be erased by the recent connections that happened during the Pleistocene (Figure 3 and
425 Table 2), pointing to the conclusion that there has been a lack of long-term isolation. These
426 findings contrast with previous phylogenetic studies above the species level that have proposed
427 diversification as a result of dispersal events between inland and coastal basins associated with
428 mountain rearrangements during Eocene-Pliocene time period (Ribeiro, 2006; Roxo et al., 2014).
429 However, our evidence of spatial congruence and recency of divergence across coastal barriers
430 indicate that although older geologic events might have contributed to the colonization of the
431 coastal basins (Wendt, Silva, Malabarba, & Carvalho, 2019), temporary connections among the
432 coastal basins promoted during the Pleistocene cycles are the factors shaping the divergence
433 patterns observed in the genomic data. Moreover, the differences in the inferred timing of
434 divergence (i.e., temporal dissonance across species and geographic breaks) point to the episodic
435 nature of when historical connections were traversed, or conversely differences in the
436 effectiveness of barriers, which is a conclusion that is reached whether a common or a species-
437 specific mutation rate are used to estimate divergence times. Nevertheless, there is some temporal
438 clustering (e.g., LGM ~25 kya and ~100 kya; Figure 3), indicating that a null model of random
439 divergence times can be rejected (Bunnefeld, Hearn, Stone, & Lohse, 2018).

440 Irrespective of the specific cause for differences in the relative ephemerality of genetic
441 structure (i.e., among isolated basins within each of the regional groups; Figure 3), and given that
442 significant genetic structure is also observed within each division (see Figure 2), an inescapable
443 conclusion is that genetic differentiation differs substantially depending upon the geographic
444 setting. Below we discuss what the differences in the ephemerality of isolation across space, as
445 well among taxa, implies about the factors structuring riverine fish communities and communities
446 of the Atlantic Coastal Rainforest of Brazil.

447
448 Paleo-landscapes and ecological sieves

449 Although the common spatial genetic structure reinforces the idea that abiotic factors
450 structure freshwater species, and may be attributable to the constraints imposed by riverine
451 environments (Guinot & Cavin, 2015; Tedesco et al., 2012), fishes within a community might
452 exhibit different genetic patterns given their species-specific ecologies associated with different
453 habitats (Waters & BurrIDGE, 2016) or dispersal capabilities (Mather, Hanson, Pope, & Riginos,
454 2018; Radinger & Wolter, 2014). That is, although historical connections associated with abiotic
455 factors are necessary for any gene flow to occur among the current basins given that they are
456 geographically isolated, they did not necessarily serve as a general conduit for movement of the
457 entire ichthyofauna. Instead, the temporary connections may have acted as taxonomic sieves with
458 respect to realized dispersal. Indeed, the habitat generalist, *M. microlepis*, tends to have relatively
459 young divergence times (Figure 3). It is also the only taxa in which gene flow during the history
460 of divergence associated with the barriers, as opposed to a single pulse of gene flow, was the
461 most probable model (Table 2). In comparison, divergence times were relatively older, and gene
462 flow was limited to a single pulse, in the more specialized taxa that inhabit the highland or the

463 lowland rivers, as well as in the forest habitat specialist (Figure 3 and Table 2). In other words,
464 species-specific differences could reflect the general difference in isolation, or conversely
465 connectivity, such that some temporary passages were more or less accessible to some taxa as a
466 function of dispersal propensities. Under this hypothesis, ecological differences in the fish are
467 causally linked to the relative ephemerality of isolation – that is, ecology acts as a sieve,
468 determining the likelihood of dispersal. Whether the differences observed across regional
469 divisions are consistent with a given dispersal likelihood is an interesting proposition. However,
470 at this point, and given the noted differences in physical characteristics across regional divisions,
471 it is also possible that the paleo-landscapes themselves also contribute to when connections are
472 forged (see also Dolby et al., 2018).

473 How does the notion of localized and species-specific differences in isolation of these
474 riverine fish compare to our ideas about community responses of the terrestrial counterparts of
475 the Brazilian Coastal Atlantic Rainforest during the Pleistocene? A community-wide effect
476 supporting alternative scenarios have been suggested based on inferred congruence of population
477 histories associated with Pleistocene climatic changes in the Atlantic Forest (Carnaval et al.,
478 2009; Leite et al., 2016; Paz et al., 2018; but see Thomé, Zamudio, Haddad, & Alexandrino, 2014
479 for discussion about barriers in the region). In contrast, others have argued that in hyperdiverse
480 communities, like the Atlantic Rainforest, congruency in species responses will be highly
481 dependent on the degree of species interactions and ecological fitting (Bunnefeld et al., 2018).
482 Our findings indicate that aquatic organisms may exhibit species-specific divergence histories,
483 despite being under strong dispersal constraints imposed by riverine environments. Moreover,
484 and perhaps somewhat counter-intuitively, our results suggest that an ecological sieve contributes
485 to temporal dissonance in the response of taxa to temporary connections despite spatial

486 congruence, unlike conclusions about shared histories of terrestrial organisms. It may be that
487 differences in processes between riverine and terrestrial systems indeed warrant what might be
488 characterized as different perspectives on the factors structuring divergence. In fact, our
489 population-level findings add to recent evidence that freshwater fishes' species range may be
490 determined by the species' position in the river network, suggesting that theories developed for
491 open landscapes are inadequate to predict patterns in dendritic landscapes, such as rivers
492 (Carvajal-Quintero et al., 2019). At this point, however, it is not clear whether an emphasis on the
493 stability of regions, as opposed to dispersal during periods of climatic and geologic change, in
494 terrestrial versus riverine systems, respectively, is justified, or whether there might be more
495 commonalities.

496 The ramifications of the variation in the ephemerality of isolation across space, and
497 among taxa, can be extended to consideration of the speciation process and distribution of
498 diversity. For example, one of the oldest and one of the youngest divergence estimates (i.e., the
499 northern division in *H. boulengeri* and the southern division in *Hollandichthys*, respectively;
500 Figure 3) correspond to the proposed boundaries of putative species recognized by morphological
501 data (Carvalho, 2006; Bertaco & Malabarba, 2013). In addition, for *Bryconamericus*, one species
502 boundary corresponds to the southern division inferred in our study (Hirschmann, Fagundes, &
503 Malabarba, 2017); however, we note the lack of a correspondence between the designation of two
504 other species within this taxon and the regional structure inferred here (i.e., north clusters:
505 populations 40 and 41 for *B. ornateiceps* and population 42 for *B. tenuis* – see Text S1), which
506 results in a paraphyletic species under the currently proposed nomenclature. It is also notable that
507 the old divergences associated with the central division are not correlated with any obvious
508 morphological differentiation (Bertaco & Malabarba, 2013; Camelier, Menezes, Costa-Silva, &

509 Oliveira, 2018). The variation observed among taxa and geographic divisions could be viewed as
510 evidence of divergence along a speciation continuum, where differentiation might be observed in
511 a limited set of characters in some cases or across multiple traits, as expected as isolation persists
512 (see Huang & Knowles 2016b). Through this lens, differences among the taxa sampled here
513 would be consistent with differences in the degree of protraction of the speciation process,
514 (Dynesius & Jansson, 2013), and the different lineages or geographic divisions representing
515 differences in the stage of speciation (see Sukumaran & Knowles 2016), because genetic
516 structure as we show is not equivalent – it is more or less ephemeral depending on the geographic
517 setting and the given species.

518 Although the strong spatial congruence in divergence patterns across taxa suggests that
519 abiotic factors supersede any taxon-specific differences in their ecologies that might make some
520 barriers more or less effective, the temporal dissonance in divergence times and the extent of
521 gene flow demonstrates how different organisms can differentially perceive the same constraint
522 to dispersal. Overall, these findings highlight how unlikely a unique explanation to fauna
523 diversification it is and the necessity to develop specific predictions at the taxon level. Although
524 time estimates need to be interpreted with caution, the striking recency of events during
525 Pleistocene indicate the role of sea-level changes in the diversification processes in coastal areas.
526 Our work suggests the diversity observed in this hotspot may be the outcome of a complex
527 history of processes that occurred not just millions of years ago, but also includes recent
528 divergence mediated by the vagility of each taxon (e.g., species differ in the extent to which they
529 might capitalize on temporary dispersal routes during Pleistocene sea-level fluctuations).
530 Understanding the response of the organisms to these ephemeral processes, and how they drive

531 population differentiation, is critical to generate expectations on their response to future increases
532 in sea level.

533

534

535 **Acknowledgements**

536 This work was funded by Rackham Predoctoral Fellowship from the University of
537 Michigan (UM), Hubbs, Carl L. and Laura C. Fellowship from the University of Michigan
538 Museum of Zoology (UMMZ) and an Ichthyology Student Award (also from UMMZ) to ATT,
539 and by NSF Dissertation Improvement Grant DEB-15-01301 to LLK and ATT. We are very
540 thankful to Prof. Luiz R. Malabarba and the Ichthyology Laboratory at the Universidade Federal
541 do Rio Grande do Sul (UFRGS) for all logistics related to fieldwork and specimen curatorial
542 activities. We also thank all the people who contributed to fieldwork – specifically, V Bertaco, F
543 Carvalho, TP Carvalho, J Ferrer, A Hirschmann, F Jerep, G Neves, U Santos, PC Silva and J
544 Wingert, as well as Carlos Alberto Lucena and Vinícius Abilhoa from the Museu the Ciências e
545 Tecnologia, Pontifícia Universidade Católica do Rio Grande do Sul (MCP) and Museu the
546 História Natural Capão da Imbuia (MHNCI), respectively, for donating tissues for this study. In
547 addition, we thank M Kenney for help in laboratory work, Q He for assistance in analyses, and
548 TP Carvalho, R Pirani, J Prado, L Resende-Moreira, and three anonymous reviewers for feedback
549 in early versions of this manuscript.

550 **References**

- 551 Abell, R., Thieme, M.L., Revenga, C., Bryer, M., Kottelat, M., Bogutskaya, N., ... Petry, P.
552 (2008). Freshwater ecoregions of the world: a new map of biogeographic units for freshwater
553 biodiversity conservation. *BioScience*, 58, 403-414.
- 554 Akaike, H. (1974). A new look at the statistical model identification. In *Selected Papers of*
555 *Hirotsugu Akaike* (pp. 215-222). Springer, New York, NY
- 556 Albert, J.S., & Carvalho, T.P. (2011). Neogene assembly of modern faunas. In J.S. Albert & R.E.
557 Reis (Eds.), *Historical biogeography of Neotropical freshwater fishes* (pp.119-136).
558 Berkeley, CA: University of California Press.
- 559 Albert, J.S., Petry, P., & Reis, R.E. (2011). Major biogeographic and phylogenetic patterns. In
560 J.S. Albert & R.E. Reis (Eds.), *Historical biogeography of Neotropical freshwater fishes*
561 (pp.21-56). Berkeley, CA: University of California Press.
- 562 Ali, J.R., & Aitchison, J.C. (2014). Exploring the combined role of eustasy and oceanic island
563 thermal subsidence in shaping biodiversity on the Galápagos. *Journal of Biogeography*, 41,
564 1227-1241.
- 565 Avise, J.C. (1992). Molecular population structure and the biogeographic history of a regional
566 fauna: a case history with lessons for conservation biology. *Oikos*, 63, 62-76.
- 567 Azevedo, M.A. (2010). Reproductive characteristics of characid fish species (Teleostei,
568 Characiformes) and their relationship with body size and phylogeny. *Iheringia - Série*
569 *Zoologia*, 100(4), 469-482.
- 570 Bermingham, E., & Avise, J.C. (1986). Molecular zoogeography of freshwater fishes in the
571 southeastern United States. *Genetics*. 113(4), 939-965.
- 572 Bertaco, V.A., & Malabarba, L.R. (2013). A new species of the characid genus *Hollandichthys*
573 *Eigenmann* from coastal rivers of southern Brazil (Teleostei: Characiformes) with a
574 discussion on the diagnosis of the genus. *Neotropical Ichthyology*, 11(4), 767-778.
- 575 Bizerril, C.R.S.F. (1994). Análise taxonômica e biogeográfica da ictiofauna de água doce do leste
576 brasileiro. *Acta Biologica Leopoldensia*. 16, 51-80.
- 577 Bunnefeld, L., Hearn, J., Stone, G.N., & Lohse, K. (2018). Whole-genome data reveal the
578 complex history of a diverse ecological community. *Proceedings of the National Academy of*
579 *Sciences*. 115(28), E6507-E6515.
- 580 Burbrink, F.T., Chan, Y.L., Myers, E.A., Ruane, S., Smith, B.T., & Hickerson, M.J. (2016).
581 Asynchronous demographic responses to Pleistocene climate change in Eastern Nearctic
582 vertebrates. *Ecology Letters*, 19(12), 1457-1467.
- 583 BurrIDGE, C.P., Craw, D., & Waters, J.M. (2006). River capture, range expansion, and
584 cladogenesis: the genetic signature of freshwater vicariance. *Evolution*, 60, 1038-1049.
- 585 Camelier, P., Menezes, N.A., Costa-Silva, G.J., & Oliveira, C. (2018). Molecular phylogeny and
586 biogeographic history of the Neotropical tribe *Glandulocaudini* (Characiformes: Characidae:
587 *Stevardiinae*). *Neotropical Ichthyology*, 16(1), e170157.
- 588 Catchen, J., Hohenlohe, P., Bassham, S., Amores, A., & Cresko, W. (2013). Stacks: an analysis
589 tool set for population genomics. *Molecular Ecology*, 22(11), 3124-3140.
- 590 Carnaval, A.C., Hickerson, M.J., Haddad, C.F., Rodrigues, M.T., & Moritz, C. (2009). Stability
591 predicts genetic diversity in the Brazilian Atlantic forest hotspot. *Science*, 323(5915), 785-
592 789.
- 593 Carvajal-Quintero, J., Villalobos, F., Oberdorff, T., Grenouillet, G., Brosse, S., Huguény, B., ... &
594 Tedesco, P. A. (2019). Drainage network position and historical connectivity explain global

595 patterns in freshwater fishes' range size. *Proceedings of the National Academy of Sciences*,
596 201902484.

597 Carvalho, F.R. (2006). *Taxonomia das populações de Hyphessobrycon boulengeri (Eigenmann,*
598 *1907) e Hyphessobrycon reticulatus Ellis, 1911 (Characiformes: Characidae)* (Master
599 *thesis)*. UNESP, Brazil

600 Carvalho, M. L., Oliveira, C., Navarrete, M. C., Froehlich, O., & Foresti, F. (2002). Nuclear
601 DNA content determination in Characiformes fish (Teleostei, Ostariophysi) from the
602 Neotropical region. *Genetics and Molecular Biology*, 25(1), 49-55

603 Chakona, A., Swartz, E.R., & Gouws, G. (2013). Evolutionary drivers of diversification and
604 distribution of a southern temperate stream fish assemblage: testing the role of historical
605 isolation and spatial range expansion. *PloS one*, 8, e70953.

606 Chifman, J., & Kubatko, L. (2014). Quartet inference from SNP data under the coalescent model.
607 *Bioinformatics*, 30, 3317-3324.

608 Conti, L.A., & Furtado, V.V. (2009). Topographic registers of paleo-valleys on the southeastern
609 Brazilian continental shelf. *Brazilian Journal of Oceanography*, 57(2), 113-121.

610 Dias, M.S., Oberdorff, T., Hugueny, B., Leprieur, F., Jézéquel, C., Cornu, J.F., ... Tedesco, P.A.
611 (2014). Global imprint of historical connectivity on freshwater fish biodiversity. *Ecology*
612 *Letters*, 17, 1130-1140.

613 Dolby, G.A., Ellingson, R.A., Findley, L.T., & Jacobs, D.K. (2018). How sea level change
614 mediates genetic divergence in coastal species across regions with varying tectonic and
615 sediment processes. *Molecular ecology*, 27(4), 994-1011.

616 Donoghue, M.J., & Moore, B.R. (2003). Toward an integrative historical biogeography.
617 *Integrative and comparative biology*, 43(2), 261-270.

618 Dynesius, M., & Jansson, R. (2013). Persistence of within- species lineages: a neglected control
619 of speciation rates. *Evolution* 68, 923-934.

620 Earl, D.A., & vonHoldt, B.M. (2012). STRUCTURE HARVESTER: a website and program for
621 visualizing STRUCTURE output and implementing the Evanno method. *Conservation*
622 *Genetics Resources*, 4(2), 359-361.

623 Edwards, S., & Beerli, P. (2000). Perspective: gene divergence, population divergence, and the
624 variance in coalescence time in phylogeographic studies. *Evolution*, 54, 1839-1854.

625 Edwards, D.L., Keogh, J.S., & Knowles, L.L. (2012). Effects of vicariant barriers, habitat
626 stability, population isolation and environmental features on species divergence in the
627 south- western Australian coastal reptile community. *Molecular Ecology*, 21, 3809-3822.

628 Evanno, G., Regnaut, S., & Goudet, J. (2005). Detecting the number of clusters of individuals
629 using the software STRUCTURE: a simulation study. *Molecular Ecology*, 14, 2611-2620.

630 Excoffier, L., Dupanloup, I., Huerta-Sánchez, E., Sousa, V.C., & Foll, M. (2013). Robust
631 demographic inference from genomic and SNP data. *PLoS Genetics*, 9(10), e1003905.

632 Excoffier, L., & Foll, M. (2011). Fastsimcoal: a continuous-time coalescent simulator of genomic
633 diversity under arbitrarily complex evolutionary scenarios. *Bioinformatics*, 27, 1332-1334.

634 Guinot, G., & Calvin, L. (2015). Constrasting "fish" diversity dynamics between marine and
635 freshwater environments. *Current Biology*, 25, 2314-2318.

636 He, Q., Edwards, D.L., & Knowles, L.L. (2013). Integrative testing of how environments from
637 the past to the present shape genetic structure across landscapes. *Evolution*, 67(12), 3386-
638 3402.

- 639 He, Q., & Knowles, L.L. (2016). Identifying targets of selection in mosaic genomes with machine
640 learning: applications in *Anopheles gambiae* for detecting sites within locally adapted
641 chromosomal inversions. *Molecular ecology*, 25(10), 2226-2243.
- 642 Hirschmann, A., Fagundes, N.J., & Malabarba, L.R. (2017). Ontogenetic changes in mouth
643 morphology triggers conflicting hypotheses of relationships in characid fishes (Ostariophysi:
644 Characiformes). *Neotropical Ichthyology*, 15(1).
- 645 Huang, H., & Knowles, L.L. (2016a). Unforeseen consequences of excluding missing data from
646 next-generation sequences: simulation study of RAD sequences. *Systematic Biology*, 65(3),
647 357-365.
- 648 Huang, J.P., & Knowles, L.L. (2016b) The species versus subspecies conundrum: quantitative
649 delimitation from integrating multiple data types within a single Bayesian approach in
650 *Hercules* beetles. *Systematic Biology*, 65(4), 685-699.
- 651 Irwin, D.E. (2002). Phylogeographic breaks without geographic barriers to gene flow. *Evolution*,
652 56, 2383-2394.
- 653 Knowles, L.L., & Carstens, B.C. (2007) Estimating a geographically explicit model of population
654 divergence. *Evolution*, 61, 477-493
- 655 Kopelman, N.M., Mayzel, J., Jakobsson, M., Rosenberg, N.A., & Mayrose, I. (2015). Clumpak: a
656 program for identifying clustering modes and packaging population structure inferences
657 across K. *Molecular Ecology Resources*, 15, 1179-1191.
- 658 Leite, Y.L., Costa, L.P., Loss, A.C., Rocha, R.G., Batalha-Filho, H., Bastos, A.C., ... Pardini, R.
659 (2016). Neotropical forest expansion during the last glacial period challenges refuge
660 hypothesis. *Proceedings of the National Academy of Sciences*, 113(4), 1008-1013.
- 661 Lima, S.M., Berbel-Filho, W.M., Araújo, T.F., Lazzarotto, H., Tatarenkov, A., & Avise, J.C.
662 (2017). Headwater capture evidenced by paleo-rivers reconstruction and population genetic
663 structure of the armored catfish (*Pareiorhaphis garbei*) in the Serra do Mar mountains of
664 southeastern Brazil. *Frontiers in genetics*, 8, 199.
- 665 López-Urbe, M. M., Jha, S., & Soro, A. (2019). A trait-based approach to predict population
666 genetic structure in bees. *Molecular ecology*, 28(8), 1919-1929.
- 667 Lynch, M. (2010). Evolution of the mutation rate. *Trends in Genetics*, 26, 345-352.
- 668 Massatti, R., & Knowles, L.L. (2014). Microhabitat differences impact phylogeography
669 concordance of codistributed species: genomic evidence in montane sedges (*Carex* L.) from
670 the Rocky Mountains. *Evolution*, 68(10), 2833-2846.
- 671 Massatti R., & Knowles L.L. (2016). Contrasting support for alternative models of genomic
672 variation based on microhabitat preference: species-specific effects of climate change in
673 alpine sedges. *Molecular ecology*, 25(16), 3974-3986.
- 674 Mather, A.T., Hanson, J.O., Pope, L.C., & Riginos, C. (2018). Comparative phylogeography of
675 two co- distributed but ecologically distinct rainbowfishes of far- northern Australia.
676 *Journal of Biogeography*, 45(1), 127-141.
- 677 Miller, K.G., Mountain, G.S., Wright, J.D., & Browning, J.V. (2011). A 180-million record of sea
678 level and ice volume variations from continental margin and deep-sea isotopic records.
679 *Oceanography*, 24, 40-53.
- 680 Papadopoulou, A., & Knowles, L.L. (2015). Genomic tests of the species- pump hypothesis:
681 recent island connectivity cycles drive population divergence but not speciation in Caribbean
682 crickets across the Virgin Islands. *Evolution*, 69, 1501-1517.

683 Papadopoulou, A., & Knowles, L.L. (2016). Toward a paradigm shift in comparative
684 phylogeography driven by trait-based hypotheses. *Proceedings of the National Academy of*
685 *Sciences*, 113(29), 8018-8024.

686 Parchman, T.L., Gompert, Z., Mudge, J., Schilkey, F.D., Benkman, C.W., & Buerkle, C. (2012).
687 Genome- wide association genetics of an adaptive trait in lodgepole pine. *Molecular*
688 *Ecology*, 21, 2991-3005.

689 Paz, A., Spanos, Z., Brown, J.L., Lyra, M., Haddad, C., Rodrigues, M., & Carnaval, A. (2018).
690 Phylogeography of Atlantic Forest glassfrogs (*Vitreorana*): when geography, climate
691 dynamics and rivers matter. *Heredity*, 122, 545-557.

692 Pereira, T.L., Santos, U., Schaefer, C.E., Souza, G.O., Paiva, S.R., Malabarba, L.R., ... Dergam,
693 J.A. (2013). Dispersal and vicariance of *Hoplias malabaricus* (Bloch, 1794) (Teleostei,
694 Erythrinidae) populations of the Brazilian continental margin. *Journal of Biogeography*, 40,
695 905-914.

696 Peterson, B.K., Weber, J.N., Kay, E.H., Fisher, H.S., & Hoekstra, H.E. (2012). Double digest
697 RADseq: an inexpensive method for de novo SNP discovery and genotyping in model and
698 non-model species. *PloS one*, 7(5), e37135.

699 Purcell, S., Neale, B., Todd-Brown, K., Thomas, L., Ferreira, M.A., Bender, D., ... Sham, P.C.
700 (2007). PLINK: a tool set for whole-genome association and population-based linkage
701 analyses. *The American journal of human genetics*, 81(3), 559-575.

702 Pritchard, J.K., Stephens, M., & Donnelly, P. (2000). Inference of population structure using
703 multilocus genotype data. *Genetics* 155(2), 945-959.

704 R Core Team (2018). R: A language and environment for statistical computing. R Foundation for
705 Statistical Computing, Vienna, Austria. URL <https://www.R-project.org/>.

706 Radinger, J., & Wolter, C. (2014). Patterns and predictors of fish dispersal in rivers. *Fish and*
707 *Fisheries*, 15(3), 456-473.

708 Reis, R.E., Albert, J.S., Di Dario, F., Mincarone, M.M., Petry, P., & Rocha, L.A. (2016). Fish
709 biodiversity and conservation in South America. *Journal of fish biology*, 89(1), 12-47.

710 Ribeiro, A.C. (2006). Tectonic history and the biogeography of the freshwater fishes from the
711 coastal drainages of eastern Brazil : an example of faunal evolution associated with a
712 divergent continental margin. *Neotropical Ichthyology*, 4(2), 225–246.

713 Ribeiro, A.C., Lima, F.C., Riccomini, C., & Menezes, N.A. (2006). Fishes of the Atlantic
714 Rainforest of Boracéia: testimonies of the Quaternary fault reactivation within a
715 Neoproterozoic tectonic province in Southeastern Brazil. *Ichthyological Exploration of*
716 *Freshwaters*, 17(2), 157-164.

717 Roxo, F. F., Albert, J. S., Silva, G. S., Zawadzki, C. H., Foresti, F., & Oliveira, C. (2014).
718 Molecular phylogeny and biogeographic history of the armored Neotropical catfish
719 subfamilies Hypoptopomatinae, Neoplecostominae and Otothyrinae (Siluriformes:
720 Loricariidae). *PLoS One*, 9(8), e105564.

721 Shaw, K.L., & Gillespie, R.G. (2016). Comparative phylogeography of oceanic archipelagos:
722 Hotspots for inferences of evolutionary process. *Proceedings of the National Academy of*
723 *Sciences*, 113(29), 7986-7993.

724 Sukumaran, J., & Knowles, L.L. (2017). Multispecies coalescent delimits structure, not species.
725 *Proceedings of the National Academy of Sciences*, 114(7), 1607-1612.

726 Swartz, E.R., Chakona, A., Skelton, P.H., & Bloomer, P. (2014). The genetic legacy of lower sea
727 levels: does the confluence of rivers during the last glacial maximum explain the

728 contemporary distribution of a primary freshwater fish (*Pseudobarbus burchelli*, Cyprinidae)
729 across isolated river systems?. *Hydrobiologia*, 726(1), 109-121.

730 Swofford, D.L. (2003). PAUP*. Phylogenetic Analysis Using Parsimony (*and Other Methods).
731 Version 4. Sinauer Associates, Sunderland, Massachusetts.

732 Tedesco, P.A., Leprieur, F., Huguény, B., Brosse, S., Dürr, H.H., Beauchard, O., ... Oberdorff, T.
733 (2012). Patterns and processes of global riverine fish endemism. *Global Ecology and*
734 *Biogeography*, 21(10), 977-987.

735 [Thomaz, A. & Knowles, L.L. \(2020\). Common passages, but temporal dissonance: genomic tests](#)
736 [suggest ecological and paleo-landscape sieves structure a coastal riverine fish community,](#)
737 [Dryad, Dataset, <https://doi.org/10.5061/dryad.zkh18936g>](#)

738 Thomaz, A.T., Malabarba, L.R., Bonatto, S.L., & Knowles, L.L. (2015). Testing the effect of
739 palaeodrainages versus habitat stability on genetic divergence in riverine systems: study of a
740 Neotropical fish of the Brazilian coastal Atlantic Forest. *Journal of Biogeography*, 42(12),
741 2389-2401.

742 Thomaz, A.T., Malabarba, L.R., & Knowles, L.L. (2017). Genomic signatures of paleodrainages
743 in a freshwater fish along the southeastern coast of Brazil: genetic structure reflects past
744 riverine properties. *Heredity*, 119(4), 287.

745 Thomaz, A.T., & Knowles, L.L. (2018). Flowing into the unknown: inferred paleodrainages for
746 studying the ichthyofauna of Brazilian coastal rivers. *Neotropical Ichthyology*, 16(3).

747 Thomé, M.T.C., Zamudio, K.R., Haddad, C.F., & Alexandrino, J. (2014). Barriers, rather than
748 refugia, underlie the origin of diversity in toads endemic to the Brazilian Atlantic Forest.
749 *Molecular Ecology*, 23(24), 6152-6164.

750 Tschá, M.K., Baggio, R.A., Marteleto, F.M., Abilhoa, V., Bachmann, L., & Boeger, W.A. (2017).
751 Sea- level variations have influenced the demographic history of estuarine and freshwater
752 fishes of the coastal plain of Paraná, Brazil. *Journal of fish biology*, 90(3), 968-979.

753 Villwock, J.A., Lessa, G.C., Suguio, K., Angulo, R.J., & Dillenburg, S.R. (2005). Geologia e
754 geomorfologia de regiões costeiras. *Quaternário do Brasil*, 378, 94-113.

755 Waters, J.M., & Burrige, C.P. (2016). Fine- scale habitat preferences influence within- river
756 population connectivity: a case- study using two sympatric New Zealand Galaxias fish
757 species. *Freshwater Biology*, 61, 51-56.

758 Weitzman, S.H., Menezes, N.A., & Weitzman, M.J. (1988) Phylogenetic biogeography of the
759 Glandulocaudini (Teleostei: Characiformes, Characidae) with comments on the distributions
760 of other freshwater fishes in eastern and southeastern Brazil. In: P.E. Vanzolini & Heyer
761 W.R. (Eds.). *Proceedings of a workshop on neotropical distribution patterns* (pp.379-427).
762 Rio de Janeiro, Brazil: Academia Brasileira de Ciências.

763 Wendt, E.W., Silva, P.C., Malabarba, L.R., & Carvalho, T.P. (2019). Phylogenetic relationships
764 and historical biogeography of *Oligosarcus* (Teleostei: Characidae): Examining riverine
765 landscape evolution in southeastern South America. *Molecular phylogenetics and evolution*,
766 140, 106604.

767 Zalán, P.V., & Oliveira J.A. (2005) Origem e evolução estrutural do Sistema de Riftes
768 Cenozóicos do Sudeste do Brasil. *Boletim de Geociências da PETROBRAS*, 13(2), 269-300.

769

770 **Data Accessibility and Availability Statement**

771 RADseq data are archive on Sequence Read Archive (SRA; BioProject ID: PRJNA 598706). All
772 post-STACKS processing files that were used as input files and main output files from analyses,
773 plus custom scripts used are available in the Dryad digital repository (doi:
774 [10.5061/dryad.zkh18936g](https://doi.org/10.5061/dryad.zkh18936g)) and on GitHub
775 (https://github.com/ichthya/ThomazKnowles2020_scripts).

776

777 **Author contributions**

778 ATT and LLK conceived the study. ATT collected the samples, performed the laboratory work,
779 and analyses. ATT and LLK wrote the manuscript.

780

781 No conflict of interest.

782

783 TABLES

784

785 **Table 1.** Results of hierarchical STRUCTURE analyses, with the full dataset (All) and the
786 population subsets (North and South) for each species. For each analysis (i.e., row), the first and
787 second most probable K-values identified using Evanno's method are reported along with the
788 correspondent ΔK . The total number of loci and individuals analyzed are given, as well as the
789 total individual genotyping rate (Gen. rate).

790

Taxa	Level	Loci	Inds.	Gen. rate	K tested	1st K	ΔK	2nd K	ΔK
M. microlepis	All	1,800	113	0.79	10	2	9,054.0	4	20.0
	North	1,042	59	0.87	5	2	5,780.7	4	1,155.1
	South	1,441	54	0.88	5	2	2,110.3	3	2,078.7
H. boulengeri	All	6,129	134	0.86	10	4	34.3	2	3.0
Hollandichthys	All	6,902	142	0.87	5	2	19,511.8	3	5.9
	North	6,536	83	0.89	5	2	7,272.8	3	2.7
	South	6,335	59	0.87	5	2	12,095.1	3	885.9
Bryconamericus	All	4,276	69	0.95	10	2	10,261.1	3	144.3
	North	4,205	34	0.95	5	2	3,960.4	4	6.0
	South	4,180	28	0.95	5	2	3,331.4	3	998.2

791

792 **Table 2.** Point estimates of demographic parameters for the more probable model of divergence with gene flow (GF) or a pulse
793 of gene flow (Pulse GF) with symmetric (sym.) or asymmetric migration (asym.) for each taxon and shared geographic divisions
794 from FASTSIMCOAL2. Specifically, ancestral population size, N_{ANC} , the population size for the northern population of each
795 division, N_2 , the migration rate, MIG as one or two parameters depending on the model, divergence time, T_{DIV} , and the time of
796 the gene flow, T_{GF} , for Pulse GF scenario are reported. Note that the population size of the southern population per geographic
797 division, N_1 , was calculated directly from the empirical data (i.e., it is a fixed parameter in the model) to improve the accuracy of
798 the other parameters estimated from the SFS (following the recommendations for the program; see Excoffier & Foll, 2011). Also
799 given are the priors (top row), and the 95% confidence interval for each parameter in parentheses. T_{DIV} and T_{GF} are also shown
800 for a fixed mutation rate ($\mu = 2.19E-08$). Parameters estimated for all the models are reported in Table S5.

Geographic division	Taxa	Model	N_{ANC}	N_1^*	N_2	T_{DIV}	T_{GF}	MIG	T_{DIV}, T_{GF} (N_1 for fixed $\mu = 2.19E-08$)
		PRIORS (not bounded)	unif[1e3,1e6]	fixed parameter	unif[1e3,1e6]	unif[1e3,2e6]	unif[1e3,1.2e5] Tadm < TDIV	GF = logunif[1e-5,20]/N2 Pulse GF = unif[1e-8,0.2]	
North	M. microlepis	GF (sym.)	12262 (7345-17895)	99119	17983 (15532-22167)	28167 (23634-36008)	na	6.60E-07 (1.5e-6 - 2e-8)	29922 (102739)
	H. bouleengeri	Pulse GF (sym.)	81988 (4916-96052)	80214	35084 (29881-38740)	143341 (137538-210449)	29997 (22455-130851)	0.00077 (0.00045 - 0.0011)	133196, 47122 (68493)
Central	M. microlepis	GF (sym.)	8758 (2131-12906)	70485	26621 (22040-31162)	37170 (31757-48590)	na	1.42E-06 (1e-6 - 2e-6)	41326 (73059)
	H. bouleengeri	Pulse GF (asym.)	120106 (11120 - 127751)	50802	30536 (28324 - 33609)	233547 (121564 - 259791)	20751 (20163 - 22319)	0.945, 0.084 (0.8942 - 0.9685, 0.058 - 0.114)	180095, 17703 (43379)
	Hollandichthys**	Pulse GF (asym.)	38053 (23486 - 44788)	98214	138302 (127331 - 150833)	108770 (103740 - 130688)	9476 (7936 - 13510)	0.047, 0.043 (0.035 - 0.074, 0.035 - 0.06)	111567, 8581 (100457)
	Bryconamericus	Pulse GF (asym.)	2566 (1171 - 19360)	81933	80988 (73847 - 88983)	116180 (98890 - 127455)	12749 (10910 - 14833)	0.008, 0.12 (0.0017 - 0.0152, 0.089 - 0.139)	123032, 16114 (89041)
South	M. microlepis	GF (sym.)	7474 (6164-8050)	26432	5228 (4669-6076)	7897 (7388-9673)	na	4.43E-06 (3e-6 - 6e-6)	7981 (27397)
	H. bouleengeri	GF (asym.)	78432 (61393 - 77183)	42781	30251 (28264 - 32751)	33847 (32239 - 37948)	na	1.2e-6, 2.1e-6 (6.8e-7 - 1.6e-6, 1.4e-6 - 2.7e-6)	30695 (36530)
	Hollandichthys**	Pulse GF (asym.)	19099 (15553 - 19419)	42411	5205 (4787 - 5946)	14253 (13616 - 16956)	1092 (1033 - 1418)	0.0037, 0.0614 (0.0009 - 0.007, 0.049 - 0.081)	14795, 1206 (43379)
	Bryconamericus	Pulse GF (asym.)	14669 (1579 - 21333)	42017	66473 (61265 - 70657)	88731 (85052 - 111817)	3734 (1551 - 42769)	0.0013, 0.0077 (0.0001 - 0.0476, 0.0047 - 0.0919)	93952, 4765 (45662)

801 * Mutation rate (μ) to calculate N_1 was estimated based on genome size available for the taxa or closely related taxa (C-value): *Mimagoniates microlepis* = 2.27e-8 (C-value
802 = 1.53); *Hyphessobrycon reticulatus* = 1.87e-8 (1.15); *Bryconamericus stramineus* = 2.24e-8 (1.64); and *Hollandichthys* ("clade C") = 2.38e-8 (1.5) (Carvalho, Oliveira,
803 Navarrete, Froehlich, & Foresti, 2002).

804 ** Divergence times estimated here for *Hollandichthys* differ from Thomaz et al. (2017) because of differences in sampling design for FASTSIMCOAL2 analyses between
805 the studies (i.e., a regional analysis here, as opposed to specific paleodrainage groupings in the 2017 manuscript) and models tested.

806 FIGURE LEGENDS

807
808 **Figure 1.** Distributional map, and specimen and habitat picture of (A) *M. microlepis* (38 mm
809 standard length - SL), (B) *H. Boulengeri* (47.8 mm SL), (C) *Hollandichthys* (*H. multifasciatus*;
810 99.5 mm SL), and (D) *Bryconamericus* (*B. microcephalus*; 57 mm SL) with sampled populations
811 for genomic analyses labeled as colored dots; see small inset of South America for area of study.
812 Different colors depict main clusters of genetic differentiation obtained with hierarchical analyses
813 among populations of each species (see Figure 2 and results for details).

814
815 **Figure 2.** Estimates of population relationships and genetic clusters in (A) *M. microlepis*, (B) *H.*
816 *Boulengeri*, (C) *Hollandichthys*, and (D) *Bryconamericus*, from SVDquartets and STRUCTURE
817 analyses. Congruent patterns of divergence are emphasized by black circles with the letter
818 corresponding to the geographic break (N = North, C = Central, S = South), which are also
819 highlighted on the distributional maps (see colored dots in Figure 1). Dashed lines indicate
820 phylogenetic relationships that do not conform strictly to geographic expectation. Note the blue
821 group in South *Bryconamericus* cluster was removed from the hierarchical analysis.

822
823 **Figure 3.** Divergence time and 95% confidence interval estimated with FASTSIMCOAL2 for the
824 more probable model inferred per taxon for each geographic division (i.e., North, Central and
825 South; Table 2) along the Brazilian coast with the estimation of sea level for the same time period
826 (Miller, Mountain, Wright, & Browning, 2011).

827

828 SUPPORTING INFORMATION

829

830 **Table S1.** List of populations sampled per taxa.

831

832 **Table S2.** Sampling information and pre- and post-processing in STACKS per taxa and
833 individual.

834

835 **Table S3.** Summary of genomic libraries based on STACKS processing per taxa, including
836 summary statistics.

837

838 **Table S4.** Model comparisons based on AIC from FASTSIMCOAL2 results.

839

840 **Table S5.** Parameters estimated with FASTSIMCOAL2 per taxa for each recognized geographic
841 break along the Brazilian coast for each model tested (i.e., with gene flow and strict divergence
842 model).

843

844

845 **Figure S1.** Summary of frequency distribution of segregating sites per base-pair position for all
846 loci for each taxon (A = *M. microlepis*, B = *H. boulengeri*, C = *Hollandichthys* and D =
847 *Bryconamericus*).

848

849 **Figure S2.** Theta distribution (θ) per loci for all taxa, with the red lines indicating the upper 95
850 percentile of θ 's that were applied to remove highly variable loci from the analyses (A = *M.*
851 *microlepis*, B = *H. boulengeri*, C = *Hollandichthys* and D = *Bryconamericus*).

852

853 **Figure S3.** Heat maps for each folded joint Site Frequency Spectrum (SFS).

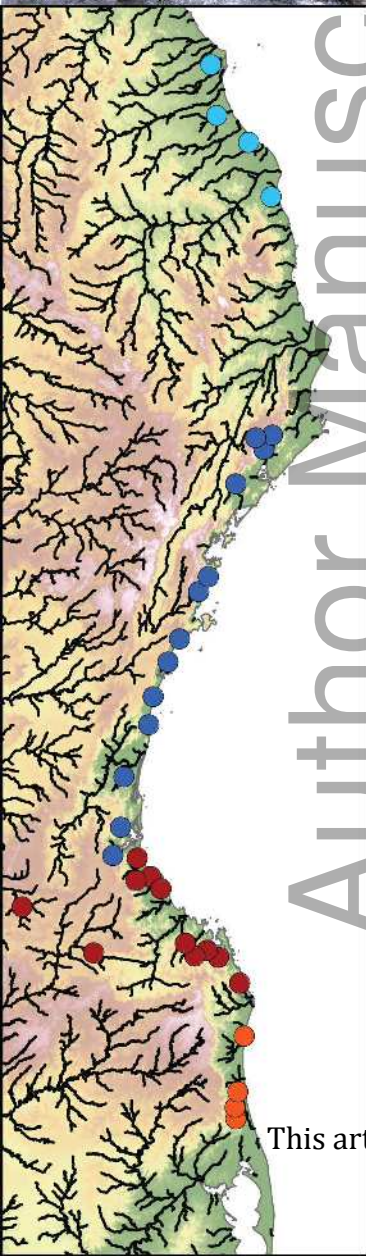
854

855 **Figure S4.** Phylogenetic trees estimated with SVDquartets at the population level for each taxon.
856 Bootstraps support values are shown on each node.

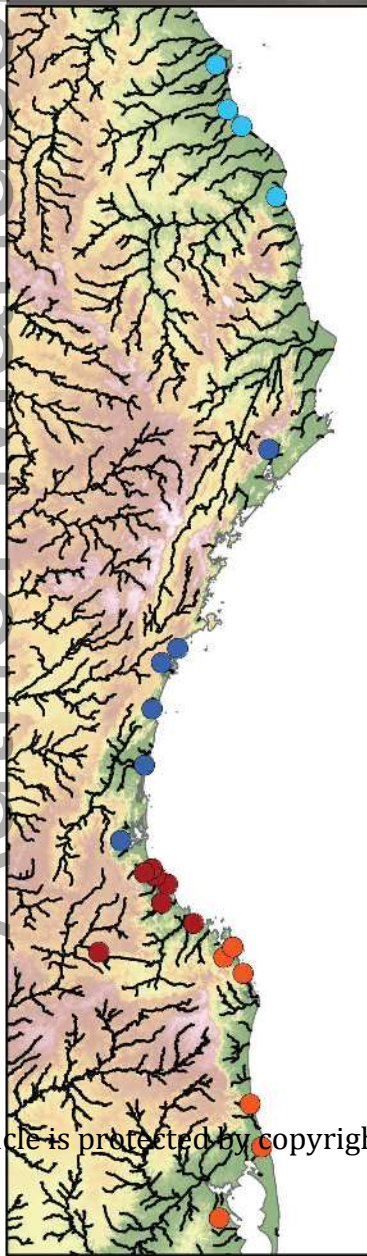
857

858

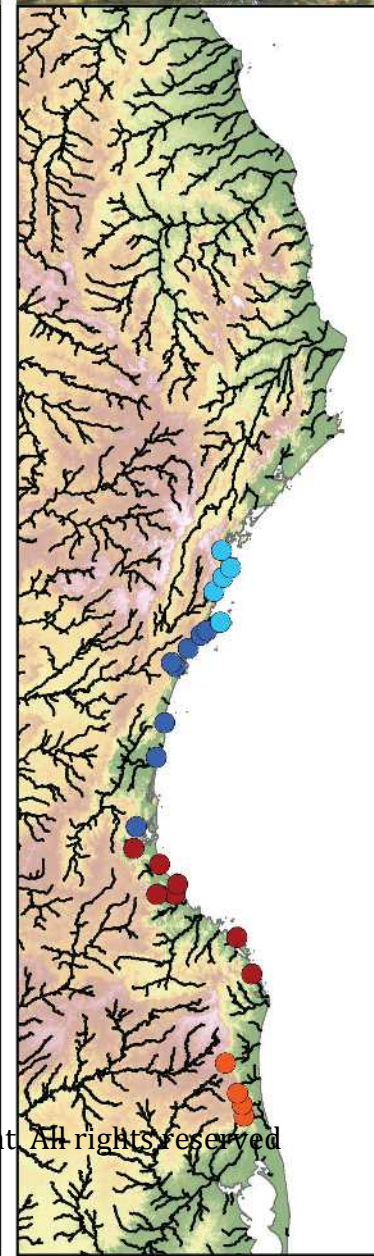
(a) *M. microlepis*



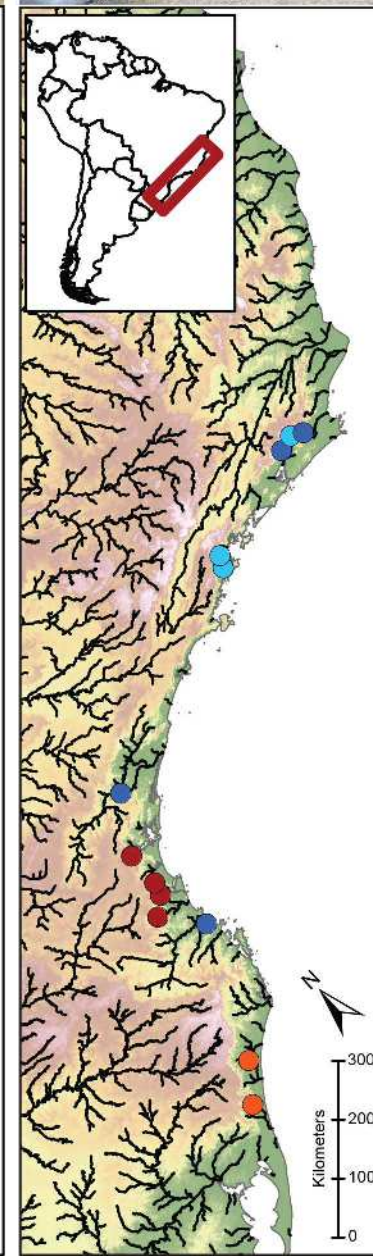
(b) *H. boulengeri*

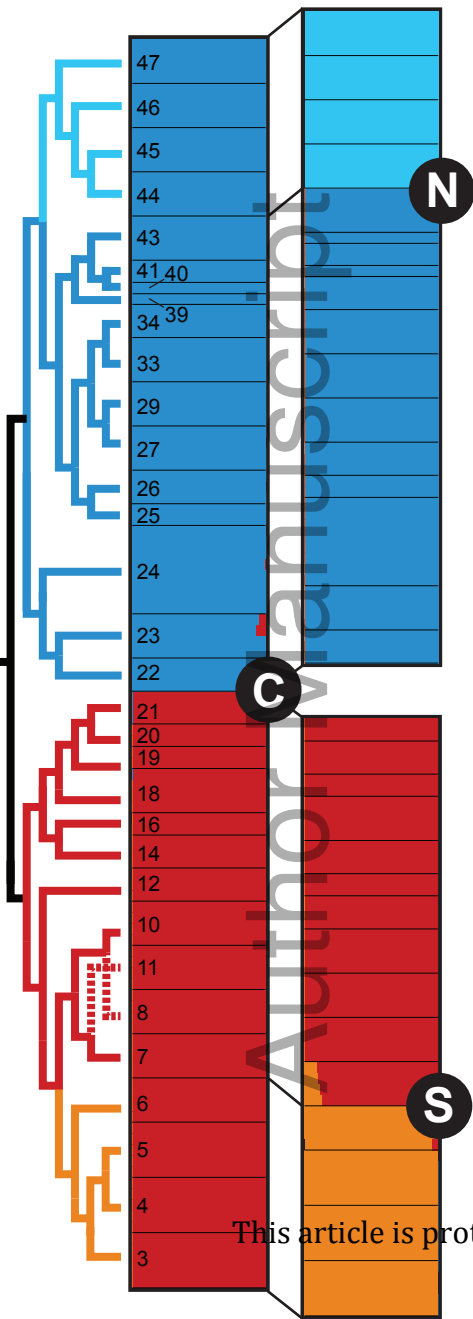
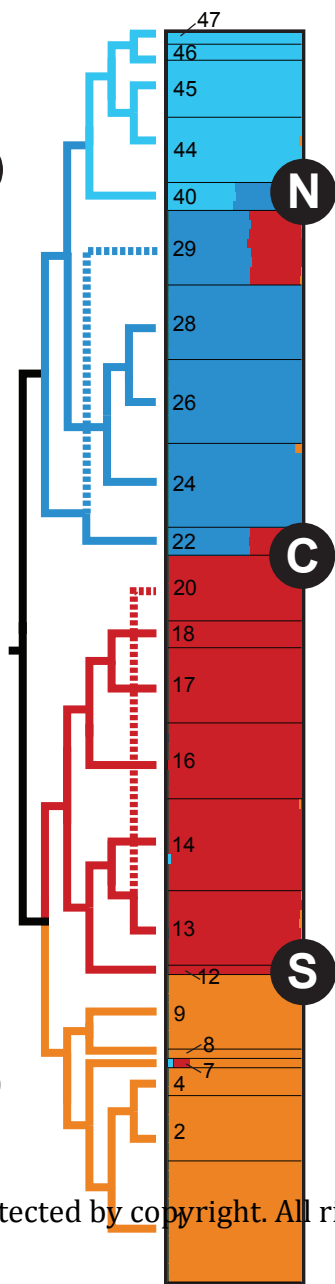


(c) *Hollandichthys*

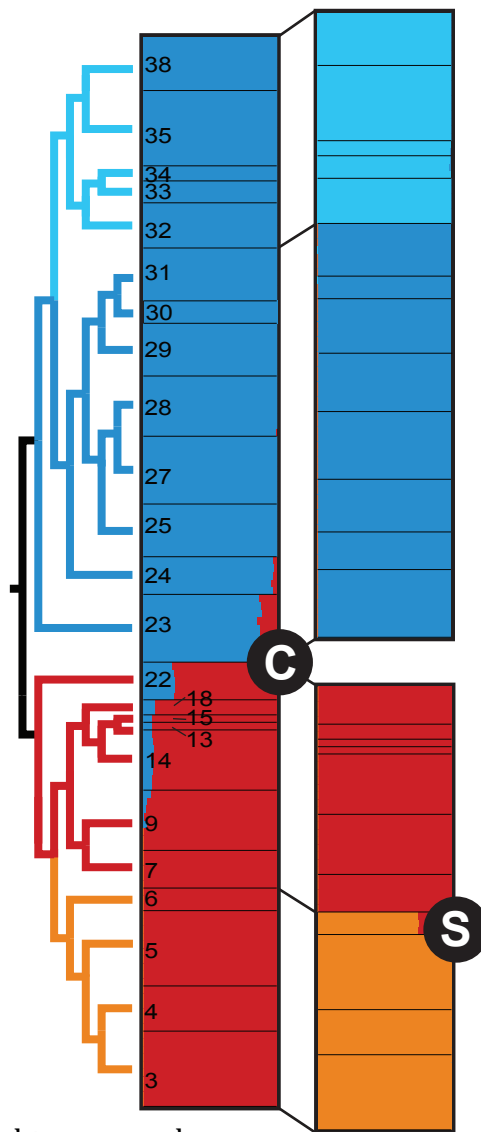
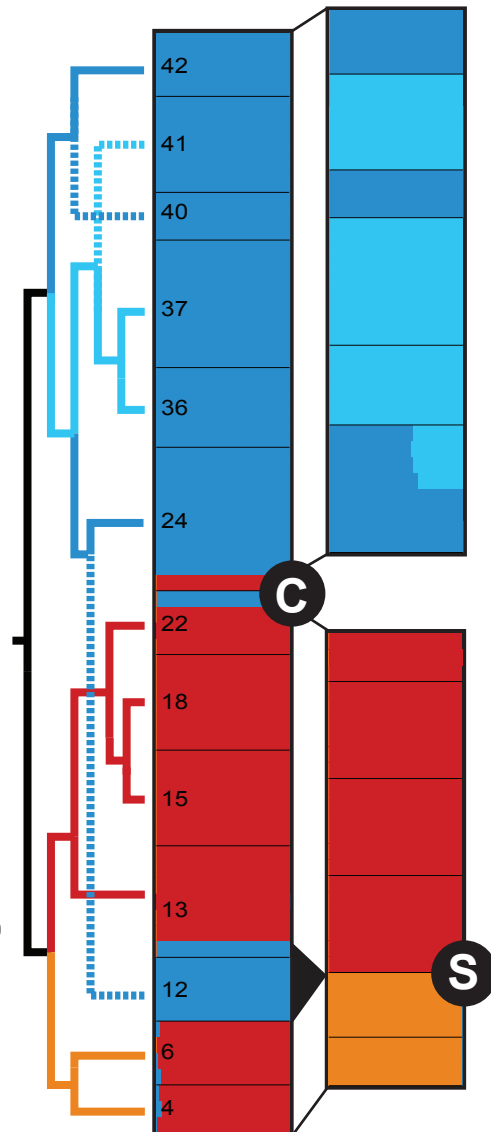


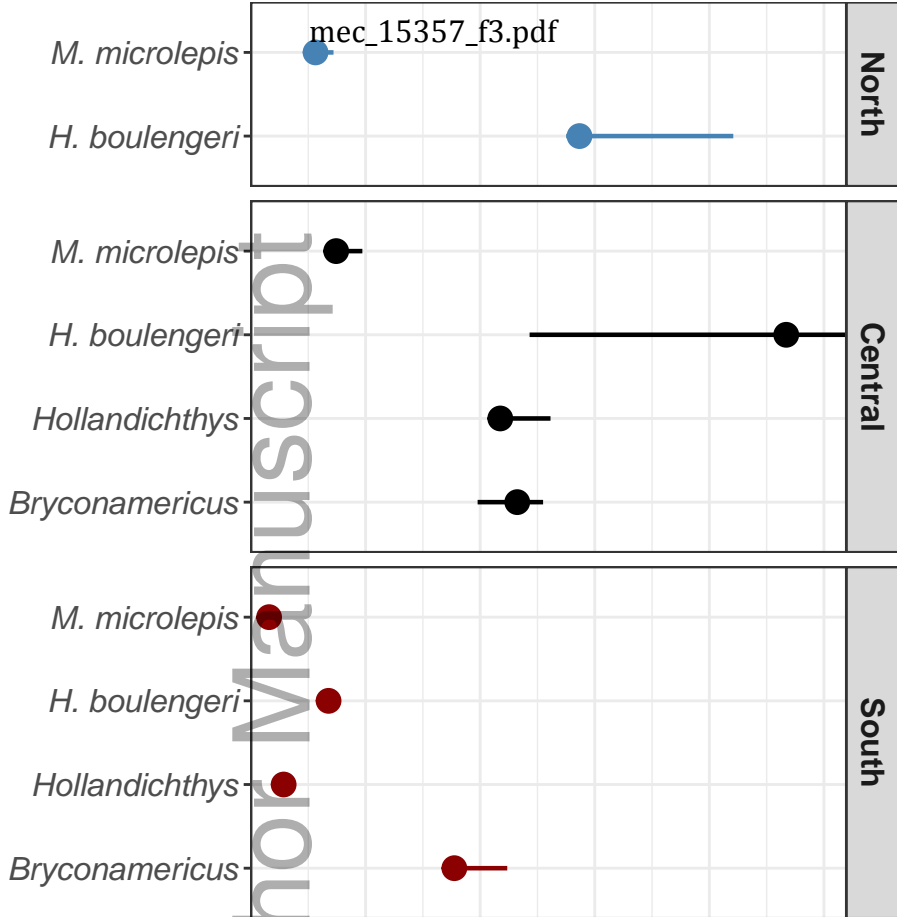
(d) *Bryconamericus*



(A)**(B)**

mec_15357_f2.pdf

(C)**(D)**

A**B**